ORIGINAL ARTICLE

대한치과의사협회지 2026; 64(7): 245-253
https://doi.org/10.22974/jkda.2026.64.7.003

Tas2r108 mediates ligand-specific bitter sensitivity and modulates longevity and metabolic health in mice

Su Young Ki[1,2], In Sun Choi[3], Kyung-Nyun Kim[3,*]

[1]Department of Pharmacology, Korea University College of Medicine, Seoul, Korea
[2]BK21 Graduate Program, Department of Biomedical Sciences, Korea University College of Medicine, Seoul, Korea
[3]Department of Physiology and Neuroscience, College of Dentistry, Kangwon National University, Gangneung, Korea

ABSTRACT

Purpose: This study aims to elucidate the physiological functions of the type 2 taste receptor 108 *(Tas2r108)*, highly expressed in the tongue and exocrine tissues, focusing on its role in bitter taste perception, metabolic homeostasis, and longevity.

Materials and Methods: To identify specific ligands, calcium imaging was performed using CHO-K1 cells transfected with *Tas2r108* and $G_{\alpha 16gust44}$. For in vivo functional analysis, a *Tas2r108* knock-out (*Tas2r108*$^{-/-}$) mouse model was generated using CRISPR/Cas9. Sensory sensitivity was evaluated through two-bottle preference tests, and long-term physiological monitoring assessed body weight, blood pressure, glucose levels, and plasma leptin concentrations.

Results: *In vitro* assays identified cycloheximide as a primary and potent ligand for *Tas2r108* compared to denatonium. In behavioral tests, *Tas2r108*$^{-/-}$ mice showed a significant reduction in bitter sensitivity to cycloheximide, demonstrating this receptor's essential role in detecting specific bitter ligands. Long-term monitoring revealed that *Tas2r108* deficiency significantly extends the average lifespan of mice. While no differences were observed in blood pressure, glucose, or total food intake, *Tas2r108*$^{-/-}$ mice exhibited greater weight gain during adulthood. Notably, plasma leptin levels were higher in the *Tas2r108*$^{-/-}$ group, correlating with this period of significant weight gain.

Conclusion: These findings demonstrate that *Tas2r108* plays a dual role in mediating ligand-specific bitter taste detection and regulating metabolic health and longevity. The results suggest that *Tas2r108* may modulate systemic homeostasis through the leptin signaling pathway, identifying it as a potential target for research into aging and metabolic regulation. ***(J Korean Dent Assoc 2026; 64(7): 245-253)***

Key words : Taste; Cycloheximide; Leptin

Introduction

Taste perception is a critical biological process that guides nutrient intake and reflects the physiological status of an organism. Proper energy and nutrient intake are essential for survival and metabolism. Among the five basic tastes, bitter taste, mediated by type 2 taste receptors (T2Rs), serves as a vital defense mechanism to avoid toxic and harmful substances[1-4]. While T2Rs were initially studied for their role in the tongue, molecular studies have revealed that these receptors are also expressed in various extra-oral tissues, suggesting they play broader physiological roles beyond simple taste detection[5-9].

In the bitter signaling pathway, T2Rs activate alpha-gustducin, leading to a cascade involving PLCβ2 and

Received Mar 30, 2026; Revised Jun 5, 2026; Accepted Jun 15, 2026

The work is supported by Basic Science Research Program through the National Research Foundation in Korea (NRF) funded by the Ministry of Science, ICT and Future Planning (2020R1F1A1049633)

*Corresponding author: Prof. Kyung-Nyun Kim
Department of Physiology and Neuroscience, College of Dentistry, Kangwon National University, Jukheon-gil 7, Gangneung, Gangwon-do 25457, Korea
Tel: +82-33-640-2450, E-mail: knkim@gwnu.ac.kr

ISSN: 0376-4672
eISSN: 2713-7961

TRPM5[10]. This results in Ca^{2+} release and Na+ influx, which depolarizes the cell and triggers ATP secretion via pannexin and CALHM1/3 to transmit signals to the nervous system[11,12]. Despite having 35 T2Rs in mice, the specific functions of individual receptors in systemic homeostasis remain largely unclarified. Among these, *Tas2r108* is particularly noteworthy due to its exceptionally high expression levels. Previous studies have shown that *Tas2r108* is expressed 2-6 times higher than GAPDH in taste papillae[13] and over 10,000 times higher in exocrine glands, such as the submandibular and lacrimal glands, compared to other T2Rs[8,14]. This unique expression pattern in exocrine tissues suggests that *Tas2r108* may function as a systemic sensor that influences metabolic health and survival.

Furthermore, metabolic homeostasis is closely linked to hormonal regulation. Leptin, a hormone proportional to body fat, acts on the hypothalamus to suppress appetite and increase energy expenditure[15]. Given the high expression of *Tas2r108* in metabolic-related exocrine organs like the pancreas and submandibular gland, it is hypothesized that this receptor may interact with systemic metabolic pathways, potentially affecting lifespan and chronic disease progression.

Therefore, the aims of this study were twofold: first, to identify the specific ligands of *Tas2r108* through intracellular Ca^{2+} activity measurements; and second, to determine its exact physiological role in vivo. Using *Tas2r108*$^{-/-}$ mice generated via CRISPR/Cas9 technology[16,17], we performed two-bottle preference tests to evaluate taste sensitivity and tracked long-term physiological indicators, including lifespan, body weight (BW), blood pressure, glucose levels, and plasma leptin. This comprehensive approach aims to elucidate the essential role of *Tas2r108* in both bitter taste detection and the maintenance of metabolic homeostasis.

Materials and methods

In vitro Ca^{2+} Imaging

CHO-K1 cells (KCLB No. 10061) were cultured in DMEM supplemented with 10% FBS and 1% penicillin-streptomycin at 37 ℃ in 5% CO_2. For *Tas2r108* expression, a chimeric construct was produced by inserting somatostatin receptor 3 and KOZAK sequences at the 5-prime end of the *Tas2r108* gene to enhance membrane localization. The gene fragment was cloned into the pcDNA3.1 expression vector using EcoRI and XhoI

Table 1. Primer sequences and structural components for *Tas2r108* cloning

Component	Sequence (5`→3`)
KOZAK	GCT AGC* GCC ACC
SSTR3	ATG GCC GCT GTT ACC TAT CCT TCA TCC GTG CCT ACG ACC TTG GAC CCT GGG AAT GCA TCC TCA GCC TGG CCC CTG GAC ACG TCC CTG GGG AAT GCA TCT GCT GGC ACT AGC CTG GCA GGA CTG GCT GTC AGT GGC
Tas2r108 Forward primer	GAA TTC† ATG CTC TGG GAA TGT ATG TAT TTG
Tas2r108 reverse primer	CTC GAG‡ CTA CTT GTA GAA ACA GAA AAT CTT CTT TGC

*: Nhe I (vector site), †: Eco R I, ‡: Xho I

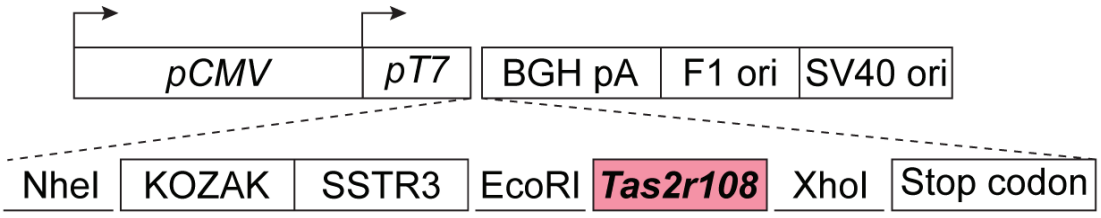

Fig. 1. Molecular cloning and heterologous expression of *Tas2r108*. Schematic shows the *Tas2r108*-inserted pcDNA3.1 expression vector. The *Tas2r108* gene (896 bp) is cloned into the mammalian expression vector pcDNA3.1 (5.5 kb).

restriction enzymes (Fig. 1). The structural components and specific primer sequences used for this cloning process, including restriction sites for *Nhe*I, *EcoR*I, and *Xho*I, are summarized in Table 1. Cells were co-transfected with *Tas2r108* and Gα16gust44 (provided by Yonsei University) using X-treme GENE HP reagent (Roche, Switzerland) at a 1:2 ratio in Opti-MEM. Expression was confirmed by RT-PCR prior to imaging. Cells seeded on cover glasses were loaded with 2mM fura2-AM and pluronic F-127 (Molecular Probes, Inc., Eugene, USA) in Ca^{2+} measurement buffer (pH 7.4) for 30 minutes at room temperature. After washing, cells were stabilized in the dark for 30 minutes. Fluorescence was measured using a CCD camera-based imaging system (Roper Scientific, USA) and MetaFluor 6.1 software. Intracellular Ca^{2+} changes (F340/F380) were recorded during perfusion of CHX (5, 50, 500 uM) and DEN (50, 150, 500 uM) at 2 ml/min. Cell viability was confirmed by 1 mM ATP treatment at the end of each session. All reagents were purchased from Sigma-Aldrich (St. Louis, MO, USA) except specifically marked.

Animals and generation of *Tas2r108* knock-out mice

All experimental procedures were approved by the Kangwon National University Animal Care and Use Committee and the Living Modified Organism Commission (GWNU-2020-24-1). C57BL/6 mice were purchased from Orient Bio Inc. (Seongnam, Korea). Mice were maintained in standard plastic cages at 23 ℃ with a 12:12 hour light/dark cycle at the Kangwon National University Animal Care Facility.

Tas2r108$^{-/-}$ mice were generated using the CRISPR/Cas9 system (Macrogen Inc., Seoul, Korea). Single guide RNAs (sgRNAs) targeting exons 1 and 2 were validated in vitro using Cas9 protein (Fig. 2A). Validated sgRNA-Cas9 complexes were microinjected into fertilized embryos obtained from pregnant mare serum gonadotropin (Daesung Microbiological Labs, Inc., Uiwang, Korea) and human chorionic gonadotropin (Daesung Microbiological Labs, Inc.)-treated female mice. F0 mosaic mice were crossed with *Tas2r108*$^{+/+}$ mice to produce F1 heterozygotes (Fig. 2B). F2 homozygotes were obtained through intercrossing F1 mice (Fig. 2B. Genotypes were confirmed by PCR of tail DNA and sequencing. The specific primers used for genotyping were as follows: forward primer (5`- TGC TCT TGG AGG AAC AGA TTC-3`) and reverse primer (5`- GTG GCC TTC ATT CAT GGA CT-3`). The PCR products were analyzed to distinguish between wild-type (1,448 bp) and knock-out (602 bp) alleles based on their respective molecular weights (Fig. 2C).

Behavioral and physiological assessments

Male *Tas2r108*$^{+/+}$ and *Tas2r108*$^{-/-}$ mice were individually housed and tested for 48 hours. Mice were provided with two 10 ml pipettes containing water and a bitter solution (CHX or DEN). Pipette positions were swapped every 24 hours to avoid side preference. Fluid intake was measured every 24 hours. The preference score was calculated as: (Bitter solution intake / Total intake) x 100.

To evaluate the long-term effects of *Tas2r108* deficiency, mice were monitored until natural death. BW, blood pressure, and blood glucose were measured every two weeks. Blood pressure was recorded from the tail artery using a non-invasive system, CODA-HT2 (Kent Scientific, Torrington, CT, USA), and glucose was measured from peripheral blood using a glucometer, Accu-Chek (Roche Diagnostics, Rotkreuz, Switzerland).

Plasma leptin levels were measured at 8, 12, 16, 20, and 24 weeks of age. Blood was collected from the jugular vein into heparin-treated tubes and centrifuged at 12,000 rpm for 25 minutes. Separated plasma was stored at -80 ℃. Leptin concentration was determined using a mouse/rat leptin ELISA kit (Cat. No. M1305, Morinaga Institute of Biological Science, Inc., Yokohama, Japan) following the manufacturer's protocol, with absorbance measured at 450 nm.

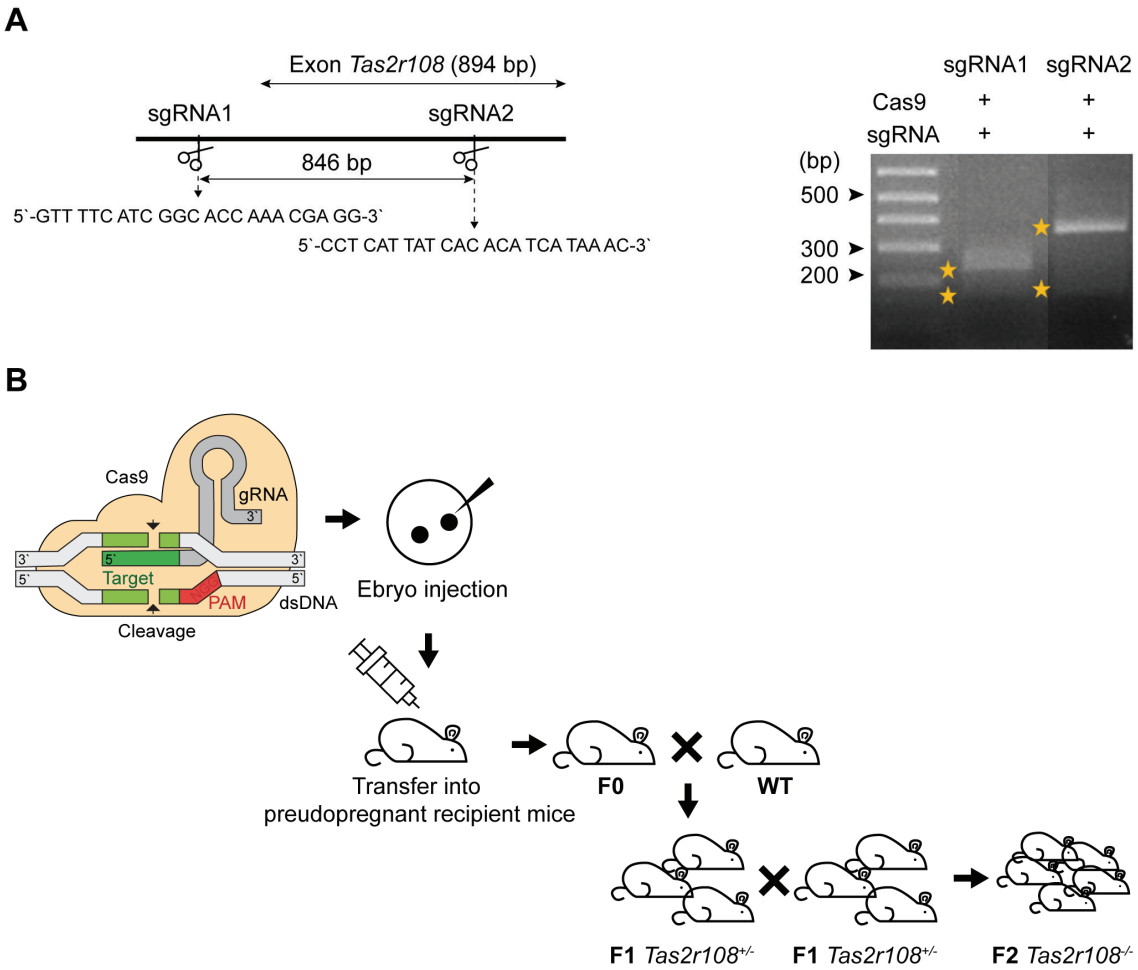

Fig. 2. Generation of *Tas2r108* knock-out mice using the CRISPR/Cas9 system. (A) Schematic represents the target site of *Tas2r108* sgRNA and its evaluation of cleavage efficiency. Electrophoresis validates the effectiveness of the sgRNA targeting the exon of the *Tas2r108* gene. (B) Schematic illustration shows the generation of *Tas2r108* knock-out (*Tas2r108*$^{-/-}$) mice. (C) PCR-based genotyping identifies F2 generation mice. The representative electrophoresis image displays PCR products from F2 mice. *Tas2r108* mosaic (+/−) F0 and wild-type (+/+) mice were crossed to obtain F1. *Tas2r108*$^{+/-}$ F1 hybrids are intercrossed to generate *Tas2r108*$^{-/-}$, *Tas2r108*$^{+/-}$, and *Tas2r108*$^{+/+}$ F2 mice.

Statistical analysis

Data were analyzed using the unpaired t test for comparisons between two groups. For concentration-dependent responses, one-way analysis of variance (ANOVA) followed by Tukey's post-hoc test was performed to determine statistical significance. All results are expressed as mean plus or minus SEM, and $p < 0.05$ was considered statistically significant.

Results

Identification of *Tas2r108* ligands via cell transfection and Ca^{2+} imaging

To verify the molecular function of the receptor, we performed in vitro signaling analysis using CHO-K1 cells. RT-PCR confirmed the expression of *Tas2r108* (896 bp) and Gα16gust44 (1,125 bp) in the transfected cells (Fig. 3A). Intracellular Ca^{2+} imaging revealed that *Tas2r108*-transfected cells exhibited robust Ca^{2+} increases in response to 5 uM and 50 uM CHX (Fig. 3B). In contrast, among the tested concentrations of DEN, only 50 uM

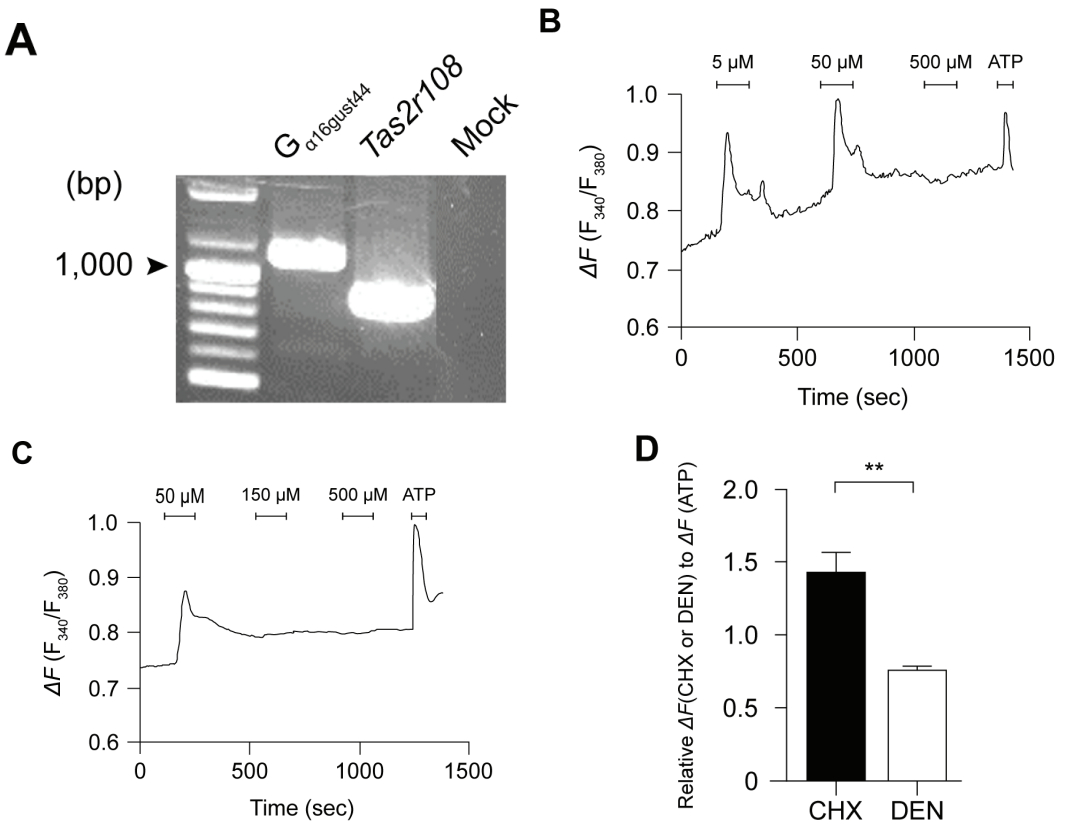

Fig. 3. Functional characterization of *Tas2r108* in a heterologous cell expression system. (A) RT-PCR analysis shows the expression of *Tas2r108* and $G_{\alpha 16gust44}$ expression in CHO-K1 cells. Lane 1, DNA size marker; Lane 2, *Tas2r108* (894 bp); Lane 3, Gα16gust44 (1,125 bp); Lane 4, non-transfected CHO-K1 cells as a negative control (Mock). (B) Representative traces show intracellular Ca^{2+} activity in response to CHX. Transfected CHO-K1 cells are loaded with fura-2 AM and stimulated with varying concentrations of CHX (5, 50, and 500 μM). (C) Representative traces show intracellular Ca^{2+} activity in response to DEN. Experimental conditions were identical to (B), with cells stimulated with 50, 150, and 500 μM DEN. (D) Quantitative analysis represents relative intracellular Ca^{2+} responses. The fluorescence changes are normalized to the response evoked by 1 mM ATP. Data are presented as mean ± SEM (**$p < 0.001$, unpaired *t*-test, n=3).

elicited a significant response (Fig. 3C). When the Ca^{2+} activity for 50 uM CHX and DEN was compared relative to the ATP-induced response, the activity for 50 uM CHX was significantly higher than that for 50 uM DEN ($p < 0.001$) (Fig. 3D). These results identify CHX as a primary and potent ligand for *Tas2r108*.

Generation and genotyping of *Tas2r108* knock-out mice

To investigate the physiological role of *Tas2r108*, we generated *Tas2r108*$^{-/-}$ mice using the CRISPR/Cas9 system. Following the microinjection of the Cas9 protein-sgRNA complex into fertilized embryos, 40 F0 generation mice were obtained. Among them, five mice (two males and three females) were identified as *Tas2r108* mosaic founders. These founders were crossed with *Tas2r108*$^{+/+}$ mice to produce F1 heterozygotes, and subsequent intercrossing of F1 mice yielded F2 offspring. The F2 generation consisted of 4 *Tas2r108*$^{+/+}$, 12 *Tas2r108*$^{+/-}$, and 6 *Tas2r108*$^{-/-}$ mice (Table 2). This distribution followed the expected Mendelian inheritance ratio, confirming the successful establishment of the *Tas2r108*$^{-/-}$ line.

Table 2. Genotype distribution of F2 generation mice generated by CRISPR/Cas9 system

F2	*Tas2r108*$^{+/+}$	*Tas2r108*$^{+/-}$	*Tas2r108*$^{-/-}$
Male	2	3	6
Female	2	9	-

Reduced Bitter Sensitivity in *Tas2r108* knock-out Mice

The effect of *Tas2r108* deficiency on bitter taste perception was evaluated using two-bottle preference tests. Notably, a significant reduction in bitter taste sensitivity was observed in *Tas2r108*$^{-/-}$ mice at a lower concentration of CHX (5 μM), where they exhibited significantly higher preference scores compared to *Tas2r108*$^{+/+}$ mice ($p < 0.001$; Fig. 4A). While both groups exhibited a concentration-dependent avoidance of CHX, the *Tas2r108*$^{-/-}$ group showed significantly higher preference scores for 50 uM CHX compared to the *Tas2r108*$^{+/+}$ group(Fig. 4A). In contrast, no significant differences were observed between 50 μM CHX and DEN within the *Tas2r108*$^{-/-}$ group (Fig. 4B), suggesting that the loss of *Tas2r108* specifically impairs the detection threshold for CHX. These findings demonstrate that *Tas2r108* is essential for maintaining high sensitivity to specific bitter ligands like CHX.

Long-term monitoring of BW and lifespan extension

Long-term physiological monitoring until natural death revealed that *Tas2r108* deficiency significantly extends the lifespan of mice. The average lifespan of *Tas2r108*$^{+/+}$ mice was 472 ± 20 days (67.4 weeks), whereas *Tas2r108*$^{-/-}$ mice survived for an average of approximately 81.0 weeks(Fig. 5A and B). This represents a statistically significant lifespan extension of about 14 weeks

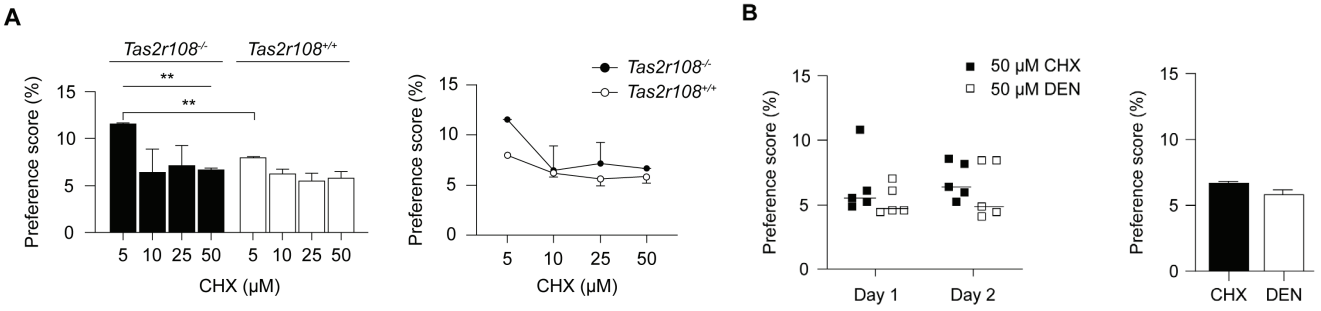

Fig. 4. Two-bottle taste preference assays for CHX and DEN in *Tas2r108*$^{-/-}$ mice. (A) Average preference scores represent 5, 10, 25, and 50 μM CHX in *Tas2r108*$^{-/-}$ and *Tas2r108*$^{+/+}$ mice. Data are presented as mean ± SEM (**$p < 0.001$, unpaired t-test; *$p < 0.01$, ANOVA). (B) Daily and average preference scores show behavior toward 50 μM CHX and DEN in *Tas2r108*$^{-/-}$ mice. Bars represent median (left) and mean ± SEM (right).

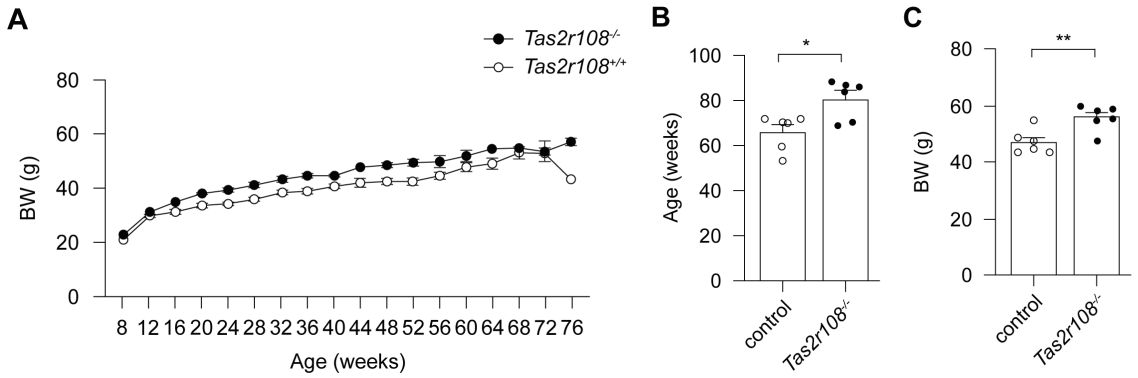

Fig. 5. Analysis of body weight (BW) and and lifespan in *Tas2r108*$^{-/-}$ mice. A. Longitudinal changes represent BW from 8 to 76 weeks of age in *Tas2r108*$^{-/-}$ and control mice. Data are presented as mean ± SEM (unpaired t-test). B. Comparison shows BW between *Tas2r108*$^{-/-}$ and control mice at 60 weeks of age. Data are presented as mean ± SEM (*$p < 0.01$, unpaired *t*-test). C. Survival analysis represents the recording of longevity in *Tas2r108*$^{-/-}$ and control mice. Data are presented as mean ± SEM (**$p < 0.001$, unpaired *t*-test).

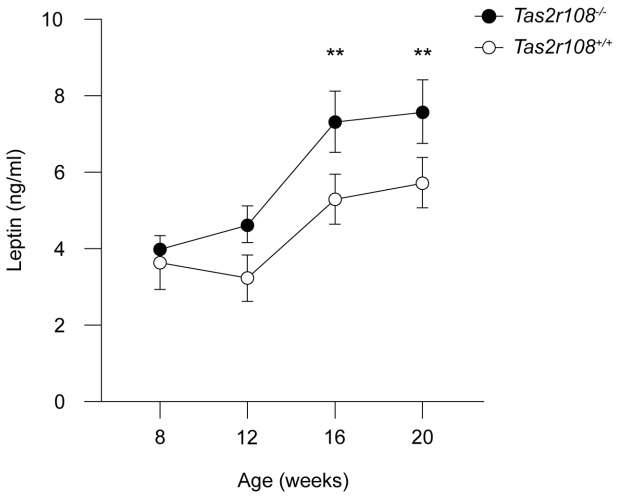

Fig. 6. Longitudinal analysis of plasma leptin levels in *Tas2r108*$^{-/-}$ and wild-type mice from 8 to 20 weeks of age. Changes in plasma leptin concentration are monitored in *Tas2r108*$^{-/-}$ and wild-type mice. Data are presented as mean ± SEM (**$p < 0.001$, unpaired t-test, n=3).

compared to the *Tas2r108*$^{+/+}$ group (Fig. 5B). Regarding BW, *Tas2r108*$^{-/-}$ mice exhibited greater weight gain between 16 and 60 weeks of age (Figs. 5A and C). Notably, both groups showed a characteristic rapid weight loss during the terminal phase of life. No adverse effects on embryonic development or reproductive capacity were observed in the *Tas2r108*$^{-/-}$ mice (data not shown).

Changes in plasma leptin levels during the lifespan

To assess the metabolic changes associated with the observed BW differences, we measured plasma leptin levels at 8, 12, 16, 20, and 24 weeks. Plasma leptin levels in *Tas2r108*$^{-/-}$ mice were significantly higher than those in *Tas2r108*$^{+/+}$ mice at the 12, 16, and 20-week marks (Fig. 6). This increase in leptin levels correlated with the period of significant weight gain observed in the *Tas2r108*$^{-/-}$ group. In contrast, no significant differences were found in blood pressure, blood glucose, or total food intake between the two groups (data not shown), suggesting that *Tas2r108* may specifically modulate systemic metabolic homeostasis and longevity through the leptin signaling pathway.

Discussion

In conclusion, our study provides a comprehensive functional characterization of *Tas2r108*, identifying it as a high-affinity receptor for CHX and DEN that serves as a critical systemic metabolic regulator. While Tas2r105 was previously identified as a CHX receptor[18], our in vitro data demonstrate that *Tas2r108* exhibits a significantly lower activation threshold, responding to concentrations as low as 5 μM. The significantly higher potency for CHX compared to DEN ($p < 0.001$) and the observed response to 50 μM DEN—a concentration far lower than the mil-

limolar ranges reported in HEK-293T systems[19,20]—suggest that *Tas2r108* functions as a specialized, high-sensitivity sensor. Interestingly, the lack of response at 500 μM CHX suggests a "bell-shaped" dose-response curve or a tight homeostatic signaling window, indicating that *Tas2r108*-mediated signaling may be subject to strict desensitization or regulatory feedback to prevent over-activation[21].

The in vivo physiological relevance of this high sensitivity was confirmed by the *Tas2r108*$^{-/-}$ mouse model. The most profound behavioral divergence between wild-type and KO mice occurred at the lowest tested concentration (5 μM CHX), where *Tas2r108*$^{-/-}$ mice failed to show typical avoidance behavior ($p < 0.001$). This identifies *Tas2r108* as the primary mediator for low-intensity bitter signals, whereas the maintenance of avoidance at higher concentrations suggests that other T2Rs provide redundant protection against toxic bitterants at high doses. Given its overwhelming expression in exocrine glands and its evolutionary conservation[22], *Tas2r108* likely exerts a systemic regulatory influence, possibly acting as a metabolic gatekeeper that modulates the expression of other type 2 taste receptors within the chromosome 6 cluster[23].

The most striking discovery of this study is the uncoupling of adiposity and mortality in *Tas2r108*$^{-/-}$ mice. Despite a 10.4% increase in body weight starting after maturity (16 weeks), these mice lived approximately 14 weeks (20%) longer than their wild-type counterparts. This phenomenon strongly supports the 'Obesity Paradox', wherein moderate weight gain in later life serves as a protective energy reservoir against aging-related frailty[24,25].

Crucially, our temporal analysis revealed that plasma leptin levels began to rise at 12 weeks, preceding the significant divergence in body weight. This temporal sequence suggests that *Tas2r108* deficiency does not simply cause obesity; rather, it directly alters the metabolic set-point or leptin secretion pathways. The elevation of leptin without a corresponding reduction in food intake indicates a state of adaptive leptin resistance or a fundamental shift in how the hypothalamus integrates metabolic signals[14,25]. The fact that this healthy obesity occurred without changes in blood pressure or glucose levels suggests that *Tas2r108*$^{-/-}$ mice maintain metabolic health despite increased adiposity. Collectively, these findings identify *Tas2r108* as a novel target for aging research, demonstrating that its modulation can decouple the negative effects of weight gain from the benefits of extended longevity.

Conflicts of Interest: None

Reference

1. 전국치과대학(원)생리학교수협의회. Physiology for dentistry. 3rd ed. Seoul: Daehan Narae Pub; 2016.
2. Nelson G, Hoon MA, Chandrashekar J, Zhang Y, Ryba NJ, Zuker CS. Mammalian sweet taste receptors. Cell 2001; 106: 381-390.
3. Tomchik SM, Berg S, Kim JW, Chaudhari N, Roper SD. Breadth of tuning and taste coding in mammalian taste buds. J Neurosci 2007; 27: 10840-10848.
4. DeFaZio RA, Dvoryanchikov G, Maruyama Y, Kim JW, Pereira E, Roper SD, et al. Separate population of receptor cells and presynaptic cells in mouse taste buds. J Neurosci 2006; 26: 3971-3980.
5. Suh HW, Lee KB, Kim KS, Yang HJ, Choi EK, Shin MH, et al. A bitter herbal medicine gentiana scabra root extract stimulates glucagon-like peptide-1 secretion and regulates blood glucose in db/db mouse. J Ethnopharmacol 2015; 172: 219-226.
6. Zhang CH, Lifshitz LM, Uy KF, Ikebe M, Fogarty KE, ZhuGe R. The cellular and molecular basis of bitter tastant-induced bronchodilation. PLoS Biol 2013; 11: e1001501.
7. Behrens M, Meyerhof W. Gustatory and extragustatory functions of mammalian taste receptors. Physiol Behav 2011; 105: 4-13.

8. Ki SY, Cho YK, Chung KM, Kim KN. An expression levels analysis of the bitter taste receptors in the murine exocrine glands. Int J Oral Biol 2018; 43: 5-11.
9. Ki SY, Jeong YT. Taste receptors beyond taste buds. Int J Mol Sci 2022; 23: 9677.
10. McLaughlin SK, McKinnon PJ, Margolskee RF. Gustducin is a taste-cell-specific G protein closely related to the transducins. Nature 1992; 357: 563-569.
11. Taruno A, Vingtdeux V, Ohmoto M, Ma Z, Dvoryanchikov G, Li A, et al. CALHM1 ion channel mediates purinergic neurotransmission of sweet, bitter and umami tastes. Nature 2013; 495: 223-226.
12. Ma Z, Taruno A, Ohmoto M, Jyotaki M, Lim JC, Miyazaki H, Niisato N, et al. CALHM3 is essential for rapid ion channel-mediated purinergic neurotransmission of GPCR-mediated tastes. Neuron 2018; 98: 547-561.
13. Choi HJ, Cho YK, Chung KM, Kim KN. Differential expression of taste receptors in tongue papillae of DBA mouse. Int J Oral Biol 2016; 41: 25-32.
14. Ki SY, Cho YK, Chung KM, Kim KN. In situ hybridization for the detection and localization of the bitter taste receptor Tas2r108 in the murine submandibular gland. Int J Oral Biol 2016; 41: 97-103.
15. Maffei M, Halaas J, Ravussin E, Pratley RE, Lee GH, Zhang Y, et al. Leptin levels in human and rodent: measurement of plasma leptin and ob RNA in obese and weight-reduced subjects. Nat Med 1995; 1: 1155-1161.
16. Ran FA, Hsu PD, Wright J, Agarwala V, Scott DA, Zhang F. Genome engineering using the CRISPR-Cas9 system. Nat Protoc 2013; 8: 2281-2308.
17. Doudna JA, Charpentier E. Genome editing. The new frontier of genome engineering with CRISPR-Cas9. Science 2014; 346: 1258096.
18. Chandrashekar J, Mueller KL, Hoon MA, Adler E, Feng L, Guo W, et al. T2Rs function as bitter taste receptors. Cell 2000; 100: 703-711.
19. Reed DR, Nanthakumar E, North M, Bell C, Bartoshuk LM, Price RA. Localization of a gene for bitter-taste perception to human chromosome 5p15. Am J Hum Genet 1999; 64: 1478-1480.
20. Foster SR, Blank K, See Hoe LE, Behrens M, Meyerhof W, Peart JN, et al. Bitter taste receptor agonists elicit G-protein-dependent negative inotropy in the murine heart. FASEB J 2014; 28: 4497-4508.
21. Lossow K, Hübner S, Roudnitzky N, Slack JP, Pollastro F, Behrens M, et al. Comprehensive analysis of mouse bitter taste receptors reveals different molecular receptive ranges for orthologous receptors in mice and humans. J Biol Chem 2016; 291: 15358-15377.
22. National Center for Biotechnology Information. HomoloGene: 49480 [Internet]. Bethesda (MD): National Center for Biotechnology Information; [cited 2019 Nov 12]. Available from: https://www.ncbi.nlm.nih.gov/homologene/49480
23. Prandi S, Voigt A, Meyerhof W, Behrens M. Expression profiling of Tas2r genes reveals a complex pattern along the mouse GI tract and the presence of Tas2r131 in a subset of intestinal Paneth cells. Cell Mol Life Sci 2018:75: 49-65.
24. Samaras TT, Storms LH, Elrick H. Longevity, mortality and body weight. Ageing Res Rev 2002; 1: 673-691.
25. Zheng H, Echave P, Mehta N, Myrskylä M. Life-long body mass index trajectories and mortality in two generations. Ann Epidemiol 2021; 56: 18-25.